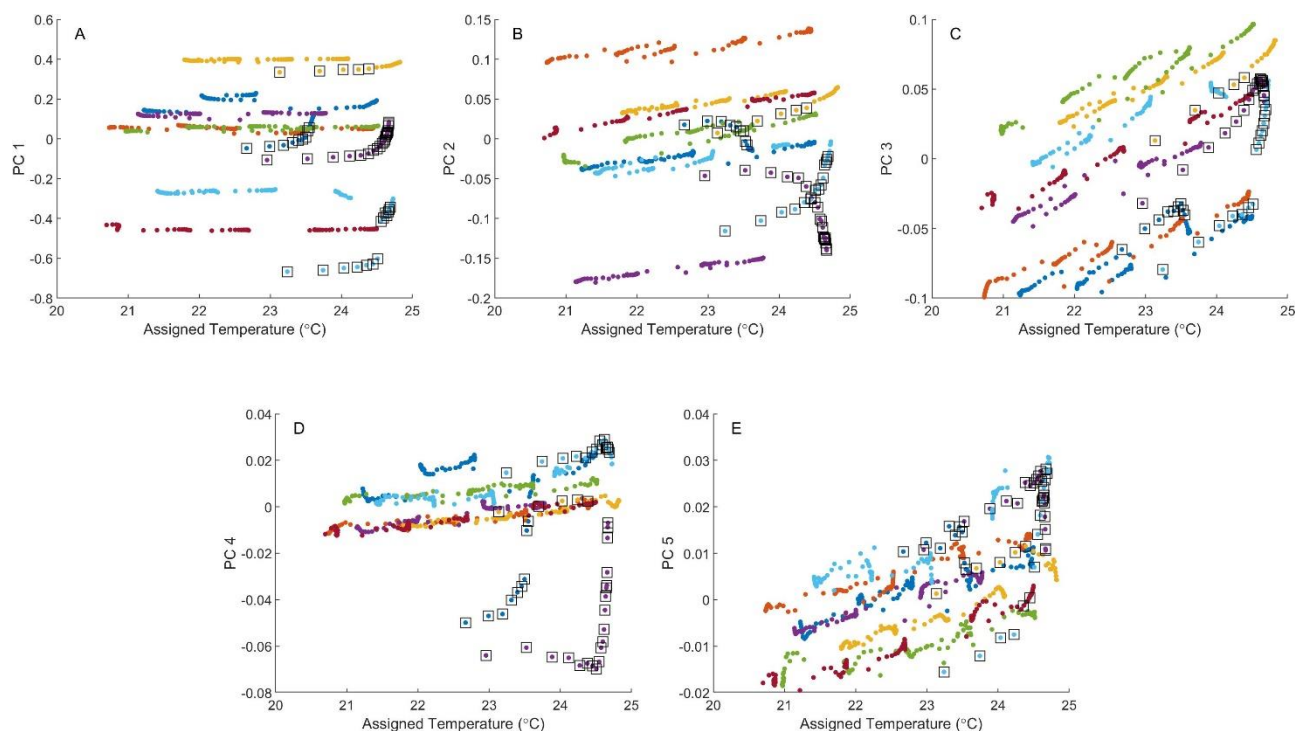


Supplemental Information

# Noninvasive Temperature Measurements in Tissue Simulating Phantoms using a Solid-State Near-Infrared Sensor



**Figure S1.** Depiction of the PCA score-temperature plots from Figure 2 while highlighting the data-points selected for removal from the overall dataset due to instabilities in the coupling between the surface of the phantom and the sensing module.

**Table S1.** provides results from a linear least-squares fit to each of the phantom datasets presented in the PCA scores – temperature plots in Figure 2. These results show measurable correlations between these PCA scores and temperature for the 2<sup>nd</sup>, 3<sup>rd</sup>, and 4<sup>th</sup> principal components. Table S1. Linear regression results for principal component scores versus temperature plots \*.

Phantom	1	2	3	4	5	6	7
Data points	91	100	95	80	100	86	100
Principal Component 1							
$\beta_1^a$	$-0.4 \pm 4$	$-4.1 \pm 0.7$	$-0.4 \pm 0.7$	$3.9 \pm 0.8$	$0.5 \pm 0.6$	$-7 \pm 1$	$-2.3 \pm 0.5$
$\beta_0^b$	$0.18 \pm 0.09$	$0.13 \pm 0.02$	$0.48 \pm 0.02$	$0.03 \pm 0.02$	$-0.07 \pm 0.01$	$-0.11 \pm 0.03$	$-0.41 \pm 0.01$
$R^2$	0.0001	0.24	0.18	0.23	0.39	0.23	0.18
Principal Component 2							
$\beta_1^a$	$9.8 \pm 0.3$	$10.4 \pm 0.3$	$1.0 \pm 0.3$	$11.6 \pm 0.2$	$15.4 \pm 0.6$	$12.4 \pm 0.5$	$13.2 \pm 0.2$
$\beta_0^b$	$-0.250 \pm 0.007$	$-0.127 \pm 0.007$	$-0.172 \pm 8$	$-0.426 \pm 0.004$	$-0.35 \pm 0.01$	$-0.32 \pm 0.01$	$-0.276 \pm 0.004$
$R^2$	0.92	0.92	0.90	0.98	0.89	0.87	0.99
Principal Component 3							
$\beta_1^a$	$17.0 \pm 0.6$	$17.2 \pm 0.4$	$18 \pm 4$	$20.3 \pm 0.4$	$20.1 \pm .04$	$18.2 \pm 0.7$	$20.5 \pm 0.3$
$\beta_0^b$	$0.47 \pm 0.01$	$-0.454 \pm 0.009$	$-0.374 \pm 0.008$	$-0.47 \pm 0.01$	$0.40 \pm 0.01$	$-0.39 \pm 0.02$	$-0.046 \pm 0.007$
$R^2$	0.91	0.95	0.97	0.97	0.96	0.88	0.98
Principal Component 4							
$\beta_1^a$	$-5.8 \pm 0.4$	$-5.3 \pm 0.1$	$-6.6 \pm 0.2$	$-6.5 \pm 0.2$	$-4.3 \pm 0.2$	$-9.3 \pm 0.5$	$-6.5 \pm 0.1$
$\beta_0^b$	$0.12 \pm 0.01$	$0.120 \pm 0.003$	$0.160 \pm 0.004$	$0.151 \pm 0.004$	$0.103 \pm 0.003$	$0.20 \pm 0.01$	$0.156 \pm 0.003$
$R^2$	0.66	0.94	0.95	0.96	0.89	0.82	0.96
Principal Component 5							
$\beta_1^a$	$0.06 \pm 0.3$	$0.4 \pm 0.1$	$0.67 \pm 0.08$	$-0.5 \pm 0.2$	$1.12 \pm 0.08$	$0.3 \pm 0.1$	$0.87 \pm 0.08$

$\beta_0^b$	$-0.010 \pm 0.008$	$-0.004 \pm 0.002$	$-0.011 \pm 0.002$	$0.017 \pm 0.004$	$-0.036 \pm 0.002$	$-0.002 \pm 0.002$	$-0.021 \pm 0.002$
$R^2$	0.0004	0.13	0.40	0.08	0.66	0.11	0.56

\* Analysis performed after removing outlier spectra. <sup>a</sup> Slope units =  $(1/^\circ\text{C}) \times 10^3$ ; <sup>b</sup>Y-intercept units = unitless.

**Table S2.** summarizes the linear regression results for plots of PCA scores versus the amount of each chemical constituent used to construction the seven phantoms. These analyses were performed on the individual phantoms as shown in Figure 4. These results reveal that the PCA scores for the 1<sup>st</sup> principal component is mostly correlated with the concentrations of water and gelatin in the phantom matrixes. Table S2. Linear regression results for scores versus phantom component concentration.

Principal Component	1	2	3	4	5
Water					
$\beta_1^a$	$-7.7 \pm 0.2$	$-0.2 \pm 0.1$	$0.83 \pm 0.06$	$0.06 \pm 0.06$	$0.010 \pm 0.009$
$\beta_0^b$	$5.1 \pm 0.1$	$0.14 \pm 0.07$	$-0.05 \pm 0.04$	$-0.042 \pm 0.009$	$0.007 \pm 0.006$
$R^2$	0.73	0.007	0.21	0.03	0.002
Gelatin					
$\beta_1^a$	$6.7 \pm 0.2$	$0.14 \pm 0.09$	$-0.79 \pm 0.05$	$-0.03 \pm 0.01$	$0.004 \pm 0.008$
$\beta_0^b$	$-1.60 \pm 0.04$	$-0.03 \pm 0.02$	$0.19 \pm 0.01$	$0.008 \pm 0.003$	$-0.001 \pm 0.002$
$R^2$	0.70	0.004	0.24	0.01	0.0004
Intralipid					
$\beta_1^a$	$-19 \pm 2$	$0.8 \pm 0.5$	$4.1 \pm 0.3$	$-0.56 \pm 0.07$	$0.12 \pm 0.04$
$\beta_0^b$	$1.9 \pm 0.2$	$-0.08 \pm 0.05$	$-0.40 \pm 0.03$	$0.054 \pm 0.007$	$-0.012 \pm 0.004$
$R^2$	0.19	0.004	0.21	0.10	0.01

<sup>a</sup> Slope units =  $(1/\text{conc}) \times 10^2$ ; <sup>b</sup>Y-intercept units = unitless.